

Surface Tension of $\text{KPO}_3\text{-WO}_3$ Melts

Vladyslav V. Lisnyak, Mykola S. Slobodyanik, and Nataliya V. Stus

Chemical Department of Kyiv National Taras Shevchenko University,
Volodymyrska Str. 64, 01033, Kyiv, Ukraine

Reprint requests to Dr. V. V. L.; Fax: +38-0-44-25-81-241; E-mail: lisnyak@chem.univ.kiev.ua

Z. Naturforsch. **63a**, 61–65 (2008); received July 7, 2007

The temperatures T_{liq} of molten $x\text{WO}_3\text{-(1-x)KPO}_3$ mixtures with a molar content between $x = 0$ and $x = 0.60$ have been determined by differential thermal analysis. The surface tension of the $x\text{WO}_3\text{-(1-x)KPO}_3$ melts in the interval from $x = 0$ to $x = 0.5$ has been measured by ring tensiometry for temperatures 10 K–20 K above the melting points, up to 1373 K. The data obtained for KPO_3 were fitted by a linear dependence on the temperature and compared with data available in the literature. The surface tension of the $x\text{WO}_3\text{-(1-x)KPO}_3$ melts was found to decrease non-monotonously with x . Three bends at $x \sim 0.15$, 0.30, and 0.45 were observed in the surface tension vs. molar fraction curve. The first and the third bends correspond to eutectic compositions; the second one is related to the formation of congruently melting $\text{K}_2\text{WO}_2\text{P}_2\text{O}_7$. Equations describing the temperature and concentration dependences of the surface tension are proposed.

Key words: Molten Salts; Differential Thermal Analysis; Surface Tension; Ring Tensiometry.

1. Introduction

For the optimization of refractory metal electrolytic deposition from molten salt a comprehensive knowledge of the physical properties of the melt is required. $\text{KF-KPO}_3\text{-WO}_3$ melts are found to be suitable for the electrodeposition of W [1]. However, the properties (as e. g. conductivity, surface tension, density and viscosity) of these melts have not been studied sufficiently, thus not yet allowing their industrial use. The objective of this paper is to report on the surface tension of the molten binary $\text{KPO}_3\text{-WO}_3$ system as one of the $\text{KF-KPO}_3\text{-WO}_3$ constituents.

2. Experimental

2.1. Preparation of Samples for Measurements

All glass samples were prepared under similar conditions from a mixture of reagent grade KPO_3 (Merck, 99.95%) and WO_3 (Aesar, 99.99%). The contribution of the components was determined from the composition $x\text{WO}_3\text{-(1-x)KPO}_3$ with a molar fraction of WO_3 in the range $x = 0.00$ to $x = 0.66$. To prepare the $x\text{WO}_3\text{-(1-x)KPO}_3$ glass with an appointed value of x each mixture was molten in a zirconium crucible at 1120–1200 K for 1 h. The crucible with the glassy product was transferred into an all-welled apparatus inserted

in a shaft furnace; then bubbling with dry O_2 gas was applied during 3 h at 1073 K to remove residual water, to homogenize the melt and to prevent a reduction of its components. In order to obtain better homogeneity, the glass was remelted several times. After that the furnace temperature was lowered to 1020 K and the melt was stored for 10 h under vacuum to degasify it. The inner volume of the system was evacuated to a pressure less than 10 Pa. Finally, the melt was quenched and the glass was transferred into an ampoule under dynamic vacuum using Schlenk's technique. The ampoules then were evacuated and sealed to prevent the adsorption of water. An X-ray powder diffraction analysis of quenched and slowly cooled melts of the $\text{KPO}_3\text{-WO}_3$ system was carried out with a Philips-1500 diffractometer operating with the $\text{CuK}\alpha$ radiation. The microstructures of the glasses were studied with a Polyvar I microscope.

2.2. Measurements of Liquids

The liquid temperatures T_{liq} of the $\text{KPO}_3\text{-WO}_3$ system were determined by means of a Q-1500 differential thermal analyzer. The mixtures $x\text{WO}_3\text{-(1-x)KPO}_3$ with $x \leq 0.56$ (corresponding to 100–200 mg in mass) were placed in covered zirconium sample holders to prevent losses of P_2O_5 . The heating and the cooling curves were registered at rates of 2.5, 5 and 10 K/min.

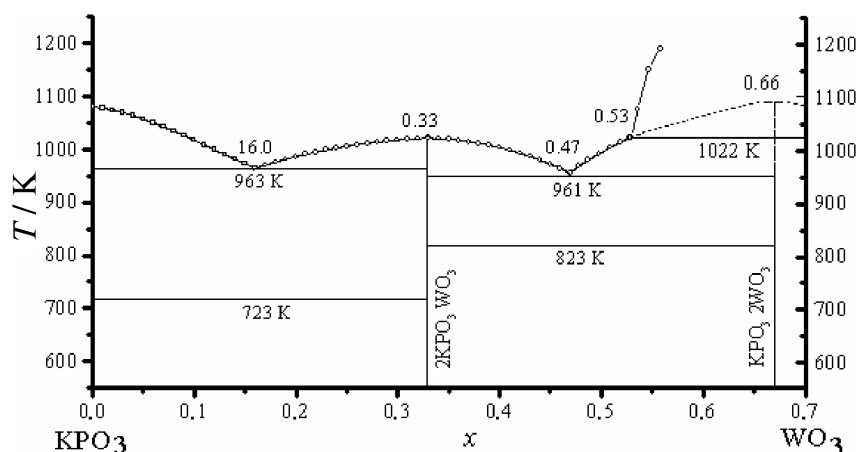


Fig. 1. Phase diagram of the KPO_3 - WO_3 system.

2.3. Measurements of Surface Tension, Apparatus and Experimental Method

The surface tension was measured in an argon atmosphere using the ring method [2–4]. All glass samples were heated to 473 K under vacuum for dehydration before use. The measurements of the surface tension have been performed with a Du Noüy tensiometer of Krüss K8 type combined with a radiofrequency induction heating shaft furnace. The tensiometer and the furnace were situated in two vertical cylindrical chambers connected by an orifice. The chambers were also connected with the vacuum line of an oil-diffusion pump and an inert gas fed system.

A zirconium crucible with a diameter of 30 mm and height of 50 mm was used as a container for the melts. The crucible was placed in a massive molybdenum crucible-like block hanging in the central part of the furnace shaft. The high thermal conductivity and the mass of the block smoothed the temperature fluctuations. Thus an isotropic thermal field was created in the central part of the massive block. The crucible with the melt under study was placed therein.

Before heating, the chamber was evacuated and filled with Ar with a pressure of 1 bar. After that the sample was heated up to the highest experimentally obtainable temperature and held for about 1 h before the first measurement was carried out as follows. A ring was immersed in the $x\text{WO}_3$ - $(1-x)\text{KPO}_3$ melts with molar fractions from $x = 0.00$ to $x = 0.50$, and then raised upwards with a rate of 1.2–12.0 mm/min. The force exerted on the ring was measured using a strain gauge. The temperature was changed in steps of 50 K from 1073 K to 1373 K with a precision ± 5 K. The

relative error of the surface tension measurement was estimated to be within $\pm 2\%$.

The temperature of the melt was measured with a Pt:Pt-Rh thermocouple assembly located around the crucible. A thermocouple of W-Re 5/20 type covered by a zirconium protector was inserted into a closed aperture of the massive block to monitor the temperature of the crucible environment. The cold ends of the thermocouples were thermostated at 273 K. To determine the surface tension γ the following equation was used:

$$\gamma = (W_{\max}gS)/[(4\pi R_0(1 + \alpha\Delta T))], \quad (1)$$

where W_{\max} is the maximal detaching force, g the gravitational constant, S the Harkins-Jordan's correction factor [5], R_0 the radius of the ring, α the linear expansion coefficient of the ring, and ΔT the difference between 298 K and the measuring temperature. Test measurements with NIST KCl standard reference material have been carried out before investigating the melts. The data obtained for the melts of the reference material agreed well with the linear equation $\gamma/(\text{mN} \cdot \text{m}^{-1}) = 179.1168 - 0.076026T/K$, for temperatures in the range $1080 \text{ K} < T < 1280 \text{ K}$ as recommended in [6]. The surface tension at 1273 K was found to be $83.02 \text{ mN} \cdot \text{m}^{-1}$, which is close to $82.33 \text{ mN} \cdot \text{m}^{-1}$ as reported in [6].

3. Results and Discussion

3.1. Phase Diagram of the KPO_3 - WO_3 System

Two compounds, $2\text{KPO}_3 \cdot \text{WO}_3$ ($\text{K}_2\text{WO}_2\text{P}_2\text{O}_7$) and $\text{KPO}_3 \cdot 2\text{WO}_3$ ($\text{KW}_2\text{O}_5\text{PO}_4$), two eutectics located at

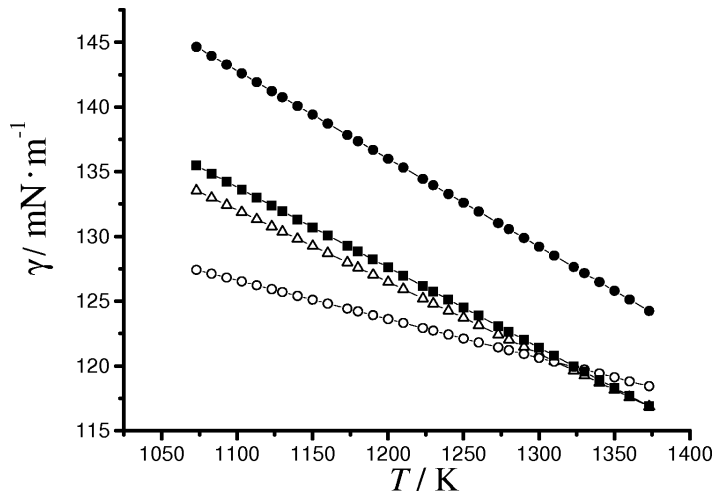


Fig. 2. Surface tensions of KPO_3 melts as a function of the temperature. The surface tension data are: open circles, [7]; black circles, [8]; open triangles, [9]; black squares, present study. The solid lines represent the least squares fitting of the data.

$x = 0.16$ (963 K) and at $x = 0.47$ (961 K), and dystectics at $x = 0.53$ (1022 K) were determined in the KPO_3 - WO_3 system according to DTA, X-ray diffraction, and microstructure analysis. Polymorphic transformations in KPO_3 and $\text{KPO}_3 \cdot 2\text{WO}_3$ were determined from the DTA and X-ray data at 723 K and at 823 K, respectively. $\text{K}_2\text{WO}_2\text{P}_2\text{O}_7$ melts congruently at (1023 ± 5) K with the corresponding enthalpy of melting equal to $11.85 \text{ kJ} \cdot \text{mol}^{-1}$. $\text{KPO}_3 \cdot 2\text{WO}_3$ melts incongruently at (1022 ± 10) K. A part of the phase diagram of the KPO_3 - WO_3 system is presented on Figure 1. The temperature T_{liq} measured by DTA can be represented by a polynomial dependence on the WO_3 mole fraction x :

$$\begin{aligned} T_{\text{liq}}(x = 0 - 0.16)/\text{K} \\ = 1081 - 204.63x - 6085.6x^2 + 17778.8x^3, \end{aligned} \quad (2)$$

$$\begin{aligned} T_{\text{liq}}(x = 0.16 - 0.33)/\text{K} \\ = 831.0 + 1085x - 1540x^2, \end{aligned} \quad (3)$$

$$\begin{aligned} T_{\text{liq}}(x = 0.33 - 0.47)/\text{K} \\ = 691.1 + 2030.4x - 3121.47x^2, \end{aligned} \quad (4)$$

$$\begin{aligned} T_{\text{liq}}(x = 0.47 - 0.53)/\text{K} \\ = -773.6 + 5965.1x - 4857.2x^2. \end{aligned} \quad (5)$$

3.2. Surface Tension of the Melts

Before studying $x\text{WO}_3$ - $(1-x)\text{KPO}_3$ melts, the temperature dependence of the surface tension γ of the KPO_3 melt was examined. It was found to vary linearly with the temperature in the range $1073 \text{ K} < T <$

1373 K according to

$$\gamma/(\text{mN} \cdot \text{m}^{-1}) = 202.0 \pm 2.5 - 0.062 \pm 0.001 T/\text{K}. \quad (6)$$

To determine the surface tensions of KPO_3 melts the ring [7] and the maximal bubble pressure [8, 9] methods were used. Literature data taken from [7–9] were extrapolated over the whole temperature range in Figure 2. The original data from the literature on the surface tension of KPO_3 [7–9] can be expressed in increasing order as

$$\begin{aligned} \gamma/(\text{mN} \cdot \text{m}^{-1}) = \\ 159.61 \pm 1.38 - 0.03 \pm 0.001 T/\text{K} [7], \end{aligned} \quad (7)$$

$$\gamma/(\text{mN} \cdot \text{m}^{-1}) = 193.2 - 0.0556 T/\text{K} [9], \quad (8)$$

$$\begin{aligned} \gamma/(\text{mN} \cdot \text{m}^{-1}) = \\ 217.6 \pm 1.4 - 0.068 \pm 0.001 T/\text{K} [8]. \end{aligned} \quad (9)$$

Our own data are close to those of Sokolova *et al.* [9], they are understated relative to Jäger's [8] data set, and they intersect the data of Williams *et al.* [7]. The data of Sokolova *et al.* [9] and ours agree well, the discrepancies being within experimental error. The deviations from the larger bubble pressure data of Jäger [8] with regard to all the shown data may be due to the neglect of Sugden's correction for non-spherical bubbles [10] in Jäger's results. The reason for the difference between the data of Williams *et al.* [7] and the other ones is not quite clear. The thermal coefficient $d\gamma/dT = -0.03 \text{ mN} \cdot \text{m}^{-1} \cdot \text{K}^{-1}$ calculated from the data of [7] [see (7)] is significantly lower than that given in [8, 9] as well as that of the present study. It

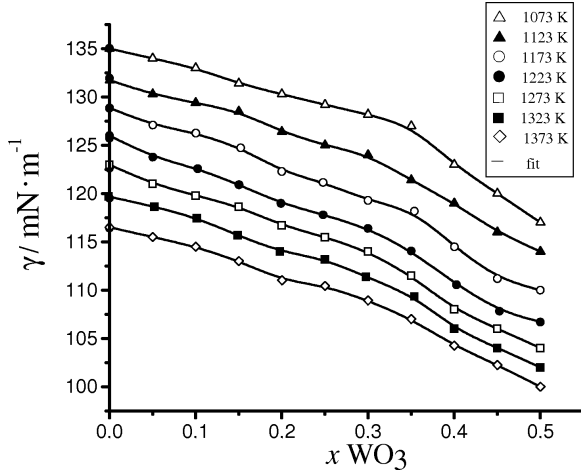


Fig. 3. Optimized values for the surface tension in the $x\text{WO}_3-(1-x)\text{KPO}_3$ melts measured at different temperatures. Open triangles, at 1073 K; black triangles, at 1123 K; open circles, at 1173 K; black circles, at 1223 K; open squares, at 1273 K; black squares, at 1323 K; open rhombs, at 1373 K. The solid lines represent the best fit of (10) to the experimental data.

is closer to $d\gamma/dT = -0.0379 \text{ mN} \cdot \text{m}^{-1} \cdot \text{K}^{-1}$ reported for the glass melts of the $\text{Na}_2\text{O}-\text{P}_2\text{O}_5$ system in [11]. Probably the composition of the glass melt, studied in [7], deviates from that of pure KPO_3 melts.

There are no data in the literature for the surface tension of pure WO_3 at temperatures close to the studied ones. The surface tension of the $x\text{WO}_3-(1-x)\text{KPO}_3$ melts are shown as a function of the molar ratio x in Figure 3. The experimental data were least-squares fitted [12] to obtain equations of the form

$$\gamma/(\text{mN} \cdot \text{m}^{-1}) = Ax + Bx^2 + Cx^3 + D. \quad (10)$$

Here x is the molar fraction of WO_3 . The obtained values for the parameters A , B , C , and D are listed in Table 1.

The measured values of the surface tension show a downward trend with increasing temperature. A power law was suggested in [12, 13] to fit the downward trend ($1073 \text{ K} < T < 1373 \text{ K}$):

$$\gamma = aT + b(10^{-5})T^2 + d, \quad (11)$$

where a , b , and d are constants and T is the temperature (Table 2).

The KPO_3 melt has a rather large surface tension due to its polymeric structure consisting of a polymetaphosphate chain and ring anions interlinked by ionic bonds between the potassium ions and the non-bridging oxygen atoms of the PO_4 tetrahedron. For

Table 1. The coefficients of (10) approximating the surface tension of the $x\text{WO}_3-(1-x)\text{KPO}_3$ melts for some chosen temperatures.

T , K	A , $\text{mN m}^{-1} \text{ mol}^{-1}$	B , $\text{mN m}^{-1} \text{ mol}^{-1}$	C , $\text{mN m}^{-1} \text{ mol}^{-1}$	D , mN m^{-1}
1073	-29.22 ± 9.0	66.48 ± 42.9	-163.79 ± 56.3	135.13 ± 0.5
1123	-14.80 ± 2.8	-40.83 ± 5.4		131.43 ± 0.3
1173	-21.40 ± 4.9	-33.28 ± 9.4		128.61 ± 0.5
1223	-24.92 ± 4.3	-27.29 ± 8.2		125.52 ± 0.5
1273	-20.70 ± 3.8	-34.00 ± 7.2		122.53 ± 0.4
1323	-18.89 ± 3.4	-33.66 ± 6.5		119.62 ± 0.4
1373	-16.75 ± 2.6	-32.08 ± 5.1		116.39 ± 0.3

Table 2. The coefficients of (11) approximating the surface tension γ of the $x\text{WO}_3-(1-x)\text{KPO}_3$ melts for selected concentrations.

x	a , $\text{mN} \cdot \text{m}^{-1} \cdot \text{K}^{-1}$	b , $\text{mN} \cdot \text{m}^{-1} \cdot \text{K}^{-2}$	d , $\text{mN} \cdot \text{m}^{-1}$
0.05	-0.15 ± 0.03	3.55 ± 1.16	251.11 ± 17.33
0.10	-0.17 ± 0.03	4.52 ± 1.12	265.43 ± 16.66
0.15	-0.15 ± 0.04	3.53 ± 1.74	250.55 ± 26.0
0.20	-0.22 ± 0.04	6.48 ± 1.76	293.40 ± 26.16
0.25	-0.25 ± 0.04	7.78 ± 1.56	309.35 ± 23.17
0.30	-0.30 ± 0.05	9.54 ± 2.0	336.13 ± 29.32
0.35	-0.35 ± 0.04	1.16 ± 0.18	367.57 ± 27.1
0.40	-0.37 ± 0.03	1.25 ± 0.14	375.19 ± 20.23
0.45	-0.39 ± 0.05	1.34 ± 0.19	381.1 ± 28.23
0.50	-0.21 ± 0.06	6.23 ± 2.4	271.88 ± 35.36

metaphosphate glasses usually only Q^2 sites (Q^n is a PO_4 tetrahedron which has n bridging and $4n$ non-bridging oxygen atoms) are registered by ^{31}P MAS NMR spectroscopy [14, 15]. Evidently minute amounts of Q^1 sites (corresponding to the terminal PO_4 tetrahedron in the chain) were observed in the KPO_3 melt as a result of the dynamic equilibrium of the polymeric phosphate anions [16].

Adding WO_3 to the KPO_3 melt leads to the formation of mixed tungstophosphate anions via gradual replacement of $\text{P}-\text{O}-\text{P}$ bonds by $\text{P}-\text{O}-\text{W}$ bridges and the appearance of additional $\text{P}-\text{O}-\text{W}$ bonds without destructing $\text{P}-\text{O}-\text{P}$ ones. Depolymerization of the polymetaphosphate anions, i. e., an increase of the Q^1 and Q^0 sites by adding the more basic oxide was confirmed by NMR measurements for numerous glass systems [15].

The dependence of the surface tension γ of the $x\text{WO}_3-(1-x)\text{KPO}_3$ melts on the concentration has shown a non-linear behaviour for all temperatures studied. The surface tension was found to decrease non-monotonously with decreasing x . Adding 50 mol% percent of WO_3 to KPO_3 decreased the surface tension to about 85% of the value for KPO_3 . Three bends at $x \sim 0.15$, 0.30 , and 0.45 , whose posi-

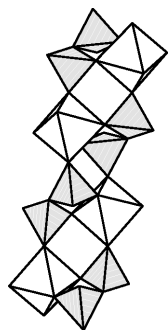


Fig. 4. Fragment of a tungstodiphosphate $[\text{WO}_2\text{P}_2\text{O}_7]_m^{2-}$ chain built from the structural data of $\text{K}_2\text{WO}_2\text{P}_2\text{O}_7$ [15].

tions correlate with the phase diagram studied, could be observed in the concentration dependence of the surface tension (see Fig. 3). The first and the third bends correspond to the eutectic compositions; the second one is related to the formation of congruently melting $\text{K}_2\text{WO}_2\text{P}_2\text{O}_7$. The crystal lattice of the compounds according to [17] is built of diphosphate groups and isolated WO_6 octahedra, having two terminal vertices; these structural units form infinite anionic chains, as represented in Figure 4.

The potassium cations are located between the tungstodiphosphate chains. The congruent melting of $\text{K}_2\text{WO}_2\text{P}_2\text{O}_7$ results in the formation of $[\text{WO}_2\text{P}_2\text{O}_7]_m^{2-}$ chain fragments in the melt. We suppose that the parameter m might decrease progressively with increasing temperature. The fragments of the $[\text{WO}_2\text{P}_2\text{O}_7]_m^{2-}$ chains should exist in the melt at $x = 0.16 - 0.47$,

i. e., in the whole composition range of crystalline $\text{K}_2\text{WO}_2\text{P}_2\text{O}_7$. Changing the WO_3 content in the melt varies to a certain extent the W/P ratio of the predominating chain fragments. For $x < 0.16$ the melt should contain WO_6 octahedra sharing the vertices with the fragments of the $[\text{PO}_3]_n^-$ chains. Here n is decreasing with x because of the incorporation of the WO_6 octahedra into the chains.

The decrease of the surface tension for all studied compositions with heating is related to an increase of the kinetic energy of the melt components and a weakening of the bonds (ionic K–O bonds interlinking complex anions composed of vertex sharing PO_4 tetrahedra and WO_6 octahedra and covalent polar P–O and W–O bonds within the anions). The weakening of the covalent polar bonds facilitates the redistribution of oxygen atoms and phosphate groups between different complex anions and causes the volatility of P_2O_5 from phosphate melts [18, 19].

Acknowledgements

The National Ministry of Science and Education of Ukraine program budgeting during the project “An influence of the composition, structure and synthetic procedure on properties of ceramic and single crystal oxide materials” (No. U01060005892) is gratefully acknowledged. The authors are in debt to Professor John Wolberg from the Technion (Haifa, Israel) for providing the Regress program.

- [1] K. Koyama, *Yoyuen* **43**, 36 (2000).
- [2] L. P. Du Nouty, *J. Gen. Physiol.* **1**, 521 (1919).
- [3] A. W. Adamson and A. P. Gast, *Physical Chemistry of Surfaces*, Wiley, New York 1997.
- [4] Y. Uchiyama and K. Kawamura, *Rev. Sci. Instr.* **49**, 543 (1978).
- [5] W. D. Harkins and H. F. Jordan, *J. Am. Chem. Soc.* **52**, 1751 (1930).
- [6] G. J. Janz, R. P. T. Tomkins, C. B. Allen, J. R. Downey, Jr., G. L. Gardner, U. Krebs, and S. K. Singer, *J. Phys. Chem. Ref. Data* **4**, 871 (1975).
- [7] D. J. Williams, B. T. Bradbury, and W. R. Maddocks, *J. Soc. Glass Technol.* **43**, 325 (1959).
- [8] F. M. Jäger, *Z. Anorg. Chem.* **101**, 1 (1917).
- [9] I. D. Sokolova, E. L. Krivovoyazov, and N. K. Voskresenskaya, *Zh. Neorg. Khim.* **8**, 2625 (1963).
- [10] S. Sugden, *J. Chem. Soc.* **121**, 858 (1922).
- [11] C. F. Callis, J. R. Van Wazer, and J. S. Metcalf, *J. Am. Chem. Soc.* **77**, 1471 (1955).
- [12] Regress program, <http://www.technion.ac.il/wolberg/regress.html>
- [13] J. Wolberg, *Data Analysis Using the Least squares Method: Extracting the Most Information from Experiments*, Springer, Berlin, Heidelberg 2006.
- [14] M. Zeyer, L. Montagne, V. Kostoj, G. Palavit, D. Prochnow, and C. Jaeger, *J. Non-Cryst. Solids* **311**, 223 (2002).
- [15] C. Mercier, G. Palavit, L. Montagne, and C. Follet-Houtteman, *C. R. Chimie* **5**, 693 (2002) and reference therein.
- [16] A. Flambard, L. Montagne, L. Delevoye, G. Palavit, J.-P. Amoureux, and J.-J. Videau, *J. Non-Cryst. Solids* **345-346**, 75 (2004).
- [17] M.-M. Borel, A. Leclaire, J. Chardon, C. Michel, and B. Raveau, *C. R. Ser. II Chem.* **324**, 189 (1997).
- [18] J. R. Van Wazer, *Phosphorus and its Compounds*, Vol. I, Interscience, New York 1958.
- [19] Yu. K. Delimarskii, *Chemistry of Ionic Melts*, Naukova dumka, Kiev 1980 (in Russian).